Priority Report

Cancer Research

Epithelial-to-Mesenchymal Transition and Autophagy Induction in Breast Carcinoma Promote Escape from T-cell–Mediated Lysis

Intissar Akalay[1], Bassam Janji[3], Meriem Hasmim[1], Muhammad Zaeem Noman[1], Fabrice André[2], Patricia De Cremoux[4], Philippe Bertheau[5], Cécile Badoual[6], Philippe Vielh[7], Annette K. Larsen[8], Michèle Sabbah[8], Tuan Zea Tan[9], Joan Herr Keira[11], Nicole Tsang Ying Hung[11], Jean Paul Thiery[9,10,11], Fathia Mami-Chouaib[1], and Salem Chouaib[1]

Abstract

Epithelial-to-mesenchymal transition (EMT) mediates cancer cell invasion, metastasis, and drug resistance, but its impact on immune surveillance has not been explored. In this study, we investigated the functional consequences of this mode of epithelial cell plasticity on targeted cell lysis by cytotoxic T lymphocytes (CTL). Acquisition of the EMT phenotype in various derivatives of MCF-7 human breast cancer cells was associated with dramatic morphologic changes and actin cytoskeleton remodeling, with $CD24^-/CD44^+/ALDH^+$ stem cell populations present exhibiting a higher degree of EMT relative to parental cells. Strikingly, acquisition of this phenotype also associated with an inhibition of CTL-mediated tumor cell lysis. Resistant cells exhibited attenuation in the formation of an immunologic synapse with CTLs along with the induction of autophagy in the target cells. This response was critical for susceptibility to CTL-mediated lysis because siRNA-mediated silencing of *beclin1* to inhibit autophagy in target cells restored their susceptibility to CTL-induced lysis. Our results argue that in addition to promoting invasion and metastasis EMT also profoundly alters the susceptibility of cancer cells to T-cell–mediated immune surveillance. Furthermore, they reveal EMT and autophagy as conceptual realms for immunotherapeutic strategies to block immune escape. *Cancer Res; 73(8); 2418–27. ©2013 AACR.*

Introduction

$CD8^+$ T cells play a crucial role in the host defenses against malignancies in both mice and humans (1). The identification of tumor-associated antigens (TAA) recognized by $CD8^+$ T lymphocytes has permitted potentiation of specific immune responses in immunotherapy strategies. Nevertheless, despite the expression of TAAs, tumor eradication by the immune system is often inefficient (2), which accounts for the disappointing clinical activity of most cancer vaccines (3). Extensive studies have shown that tumor cells themselves play a crucial role in modulating the host immune response, such that they maintain their functional disorder and evade immune surveillance (4). In this regard, it has been suggested that tumor cell growth *in vivo* is not only influenced by cytotoxic T lymphocyte (CTL) tumor cell recognition but also by tumor susceptibility to cell-mediated death (5). While the resistance of tumor cells to T-cell-mediated cytotoxicity remains a major impediment for cancer immunotherapy, its molecular basis is poorly understood.

Epithelial-to-mesenchymal transition (EMT) is a fundamental mechanism governing embryonic morphogenesis that has, intriguingly, been documented to operate in carcinomas, with the transition from an epithelial carcinoma to a mesenchymal-like state potentially linked with increased stemness, therapeutic resistance, and escape from immune surveillance (6). Snail 1 (SNAI1) is a transcription factor that induces EMT by directly repressing E-cadherin expression (7). We previously described the morphologic changes in lung cell carcinoma as a mechanism of tumor escape that was partly involved in the resistance of tumor cells to T-cell–mediated cytotoxicity (8).

Recently, autophagy has been proposed to play an important role in tumor progression and in the promotion of cancer cell death (9). Furthermore, it is shown that EMT involves the activation of several important pathways that help tumors

Authors' Affiliations: [1]Unité INSERM U753, Institut de Cancérologie Gustave Roussy; [2]U981 INSERM, Institut Gustave Roussy, Villejuif; [3]Laboratory of Experimental Hemato-Oncology, Department of Oncology, Public Research Center for Health (CRP-Sante), Luxembourg City, Luxembourg; [4]Molecular Pharmacology Unit, Institut Curie; [5]Service d'anatomie pathologique, Hôpital Saint-Louis; [6]Assistance Publique-Hôpitaux de Paris, Service d'anatomo-pathologie, Hôpital Européen Georges Pompidou; [7]Laboratoire de Recherche Translationnelle-module d'histocytopathologie; [8]Laboratory of Cancer Biology and Therapeutics, Centre de Recherche Saint-Antoine, INSERM U938 and Université Pierre et Marie Curie, Laboratoire de Recherche Translationnelle-module d'histocytopathologie, Paris France; [9]Cancer Science Institute of Singapore, [10]Biochemistry Department, National University of Singapore; and [11]Institute of Molecular and Cell Biology, A*STAR, Singapore

Note: Supplementary data for this article are available at Cancer Research Online (http://cancerres.aacrjournals.org/).

Corresponding Author: Salem Chouaib, Unité INSERM U753, Institut de Cancérologie Gustave Roussy, 114 rue Edouard Vaillant, Villejuif Cedex 94805, France. Phone: 331-4211-4547; Fax: 331-4211-5288; E-mail: chouaib@igr.fr

doi: 10.1158/0008-5472.CAN-12-2432

survive and evolve into highly invasive and metastatic variants (10). However, the relationship between EMT and autophagy-induced cell survival is unknown. Although evidence has suggested that epithelial plasticity may interfere with tumor susceptibility to cytotoxic agents, the functional consequences of EMT on T-cell–mediated cytotoxicity remain undetermined.

In this study, we sought to examine the influence of EMT on CTL-mediated lysis and its associated mechanisms and to ascertain whether EMT-induced cell plasticity could interfere with tumor cell susceptibility to this lysis. We show that EMT has functional consequences on target recognition and lysis, and we identify EMT-induced autophagy as a novel mechanism by which tumor cells regulate CTL reactivity and impede their cytotoxic activity.

Materials and Methods

T-cell clone, tumor cell lines, and culture conditions

The T-cell receptor (TCR)-Vβ13.6$^+$ Heu33 CTL clone was derived from a patient's Heu tumor as described (11). MCF-7 and derivatives were grown in Dulbecco's Modified Eagle's Media (DMEM):F12 medium supplemented with 10% heat-inactivated fetal calf serum (FCS; Gibco-BRL), 1 mmol/L sodium pyruvate (Life Technologies), and 1% penicillin/streptomycin (Life Technologies) at 37°C in a humidified atmosphere containing 5% CO_2. The MCF-7 breast cancer cell line was transfected with wild-type Snail (SNAI1), constitutively activated Snail (SNAI1-6SA) generated by mutation of Ser6 to Ala and with an empty vector, as described (12). Transfected cells were cultured in complete medium supplemented with 500 μg/mL of G418 (Life Technologies). TNF-resistant cells (2101) were derived from the TNF-sensitive human breast carcinoma MCF-7 cell line after continuous exposure to increasing doses of recombinant TNF-α (13).

Cell morphology, actin cytoskeleton, and EMT marker staining

Cell morphology images were acquired using ×20 objective by phase-contrast microscopy (Leica Microsystems). Actin filaments were stained by Alexa Fluor 488–coupled Phalloidin. EMT markers were stained with indicated antibodies and nuclei with 4′,6-diamidino-2-phenylindole (DAPI; dihydrochloride; Life Technologies). Cells were cultured in IBIDI chambers (IBIDI) and fixed with 3% paraformaldehyde for 20 minutes at room temperature. Cells were then permeabilized with 0.4% Triton X-100 and stained with indicated antibodies. Cells were analyzed with a Zeiss laser scanning confocal microscope, LSM-510 Meta (Carl Zeiss) and processed by LSM Image Examiner software (Carl Zeiss).

Western blotting

Adherent cells were lysed on the plate with lysis buffer (62.5 mmol/L Tris-HCl, pH 6.8, 2% w/v SDS, 10% glycerol, 1 mmol/L sodium orthovanadate, 2 mmol/L phenylmethylsulfonylfluoride, 25 μmol/L leupeptin, 5 mmol/L benzamidine, 1 μmol/L pepstatin, and 25 μmol/L aprotinin). Cells lysates were resolved by SDS-PAGE electrophoresis (30 μg/sample) and transferred onto nitrocellulose membranes. After incubation in blocking buffer, the membranes were probed overnight at 4°C with the primary antibodies. The labeling was visualized using peroxidase-conjugated secondary antibodies and with an ECL kit (Amersham Pharmacia Biotech). Primary antibodies against SNAI1, E-cadherin and LC3B were from Cell Signaling. Antibodies against SNAI2 and Twist were from Abcam. Antibodies against vimentin, beclin 1, and N-cadherin were from Santa Cruz Biotechnologies.

Data preprocessing of the breast cancer cell line panel

Two large breast cancer cell line datasets were established using the Affymetrix U133A or U133plus2 platform: E-TABM-157 ($n = 51$ samples corresponding to 51 cell lines) and GSE15026 ($n = 30$ samples corresponding to 19 cell lines) were downloaded from Array Express and Gene Expression Omnibus (GEO), respectively. Robust Multichip Average (RMA) normalization was conducted for each dataset. The normalized data were combined with the dataset from the present study ($n = 8$ samples from the parental MCF-7 cells, 2 Snail-expressing cell lines, and one TNF-α–resistant MCF cell line variant), and subsequently standardized using ComBat (14) to remove batch effect. The standardized data yielded a dataset of 89 samples derived from 73 cell lines.

Estimation of EMT score

An EMT scoring method was developed using ovarian carcinoma cell line expression profiling. The first step was to establish an EMT signature comparing profiles of *CDH1*- with *CDH2*-expressing cell lines using a binary regression method (BinReg; ref. 15). In the second step, the BinReg ovarian cancer EMT signature was applied to breast cancer cell lines to predict their EMT status. In the third step, the top 25% (~20 samples) with the highest probabilities for the epithelial or mesenchymal phenotype were used to obtain epithelial- or mesenchymal-specific gene lists for the breast cancer cell lines using Significance Analysis of Microarray (SAM) q value of 0 and receiver operating characteristic (ROC) value of 0.85. In the fourth step, single-sample gene set enrichment analysis (GSEA; ref. 16) was used to compute the enrichment score of a cell line based on the expression of the breast cancer cell line–specific epithelial or mesenchymal signature genes. EMT score is defined as the normalized subtraction of the mesenchymal from epithelial enrichment score. The EMT score is a precise estimate of the cell line's status as an epithelial or mesenchymal phenotype. A higher or lower EMT score indicates that the cell line exhibits a more mesenchymal or epithelial phenotype, respectively (the detailed method is submitted for publication, Tan, Huang, Thiery and Mori and colleagues).

Cytotoxicity experiments and TNF-β production assay

The cytotoxic activity of the CTL clone was measured by a conventional 4-hour ^{51}Cr release assay. Several effector:target (E:T) ratios were used on 1,000 target cells per well. Supernatants were then transferred to LumaPlate-96 wells (Perkin-Elmer), dried down, and counted on a Packard TopCount NXT. Percentage of specific cytotoxicity was calculated conventionally.

TNF-β release was detected by measuring the cytotoxicity of the culture supernatants on the TNF-sensitive WEHI-164c13 cells with an MTT colorimetric assay, as previously described (17).

Confocal microscopy analysis of immunologic synapse assembly

Tumor cells and CTLs were cocultured for 30 minutes at a 1:2 ratio. Cells were then fixed with 3% paraformaldehyde for 10 minutes and permeabilized with 0.1% (w/v) SDS solution in PBS for 10 minutes, followed by blocking with FCS 10% (v/v) solution in PBS for 20 minutes. Fixed cells were stained with an anti-phosphotyrosine monoclonal antibody (mAb) 4G10 clone (dilution 1:100, Millipore Corp.) and then with a secondary mAb coupled to Alexa Fluor 488 (Invitrogen) for 30 minutes. Cell nuclei were stained with TO-Pro 3 iodide (2 μmol/L) for 15 minutes. Analysis was conducted by a Zeiss laser scanning confocal microscope (LSM-510) and using LSM Image Examiner software (Zeiss). Conjugates formed between T cells and tumor cells were scored by visual counting. Mean number of active synapses/field were counted in 10 different fields per cell line randomly selected at ×40 magnifications. Quantification of phosphotyrosine intensity was conducted using the region measurement function of ImageJ software (NIH, Bethesda, MD).

Autophagosome detection and autophagy flux analysis

Cells were transiently transfected with 5 μg of LC3 cDNA fused with GFP (kindly provided by N. Mizuchima, Tokyo Medical and Dental University, Tokyo, Japan) using Lipofectamine 2000 (Invitrogen) according to the manufacturer's recommendation. After 48 hours, cells were cultured in IBIDI chambers (Biovalley), and the formation of autophagosomes was assessed by Zeiss laser scanning confocal microscopy LSM-510 Meta. The autophagy flux was assessed by treatment of cells for 6 hours with chloroquine (40 mmol/L), an inhibitor of the lysosomal activity, and the accumulation of the lipidated form of LC3 (LC3-II) was analyzed by Western blotting using an anti-LC3 Ab.

Immunohistochemical staining for Snail 2 and ATG5 expression

Mesenchymal and autophagic cells, respectively, were detected by SNAI2 and ATG5 staining on human breast cancer sections. Immunohistochemistry was conducted as previously described (18). The samples were incubated with mAbs against SNAI2 (Abcam) and ATG5 (MBL Japan). The signal was revealed with the DAB HistoMouse-Max Kit (Zymed Laboratories Inc.).

siRNA targeting of autophagy gene BECN1

Autophagy-defective cells were generated by transfection with *beclin1* (BECN1) siRNA. Briefly, cells were transfected by electroporation with 50 nmol of siRNA-targeting human *beclin1* (Qiagen). Luciferase (Luc) siRNA was used as a negative control. The silencing of *beclin1* was assessed by Western blotting 48 hours after transfection using appropriate antibodies.

Data mining of microarray results

Significantly regulated genes in SNAI1 or SNAI1-6SA transfectants as compared with the parental MCF-7 cells were subjected to Ingenuity Pathway Analysis (IPA). The Ingenuity database was used to identify EMT-regulated genes, whereas the dedicated autophagy database was used to extract genes involved in and/or related to the autophagic process (19, 20). IPA software was used to build a connection between EMT and the autophagy-regulated genes.

RNA isolation and SYBR green real-time quantitative PCR

Total RNA was extracted from the samples using TRIzol (Invitrogen). A total of 1 μg RNA was converted into cDNA by using Taqman Reverse transcription reagent (Applied Biosystems), and mRNA levels were quantified by SYBR-GREEN qPCR method (Applied Biosystems). Relative expression was calculated by using the comparative C_T method ($2^{-\Delta CT}$).

Flow cytometry and ALDH activity

Cells were harvested with 0.025% EDTA and double-stained with CD44 (PE) and CD24 (APC) mAbs (both from Miltenyi Biotec). Labeled cells were analyzed on a BD FACSCalibur (BD Biosciences).

ALDH activity was analyzed using the Aldefluor Assay Kit from StemCell Technologies, Inc. and following manufacturer's recommendations.

Statistical analyses

Data were analyzed with GraphPad Prism. The Student *t* test was used for single comparisons. Data were considered statistically significant when $P < 0.05$.

Results and Discussion

2101, SNAI1, and SNAI1-6SA cells display similar EMT phenotypes, but distinct EMT indicies and stemness markers

We characterized the EMT phenotype of MCF-7–derived cells that have undergone EMT following the overexpression of either wild-type Snail (SNAI1) or constitutively active Snail (SNAI1-6SA) or following the acquisition of TNF-α resistance (2101 cells). Parental MCF-7 cells exhibited a characteristic cobblestone epithelial organization with E-cadherin, β-catenin, and ZO-1 immunolocalization at cell–cell contacts that were also closely associated with cortical actin microfilaments. MCF-7 cells also expressed cytokeratin intermediate filaments, some of which were localized at sites of desmosomes. In contrast, SNAI1 and SNAI1-6SA cells displayed a spindle-like morphology with filopodia and were characterized by reduced cell–cell contacts (Fig. 1A). 2101 cells exhibited an even more extensive mesenchymal phenotype with actin microfilaments in the filopodia and lamellipodia (Fig. 1A). Immunofluorescence analysis showed a dramatic downregulation of the epithelial markers E-cadherin, β-catenin, ZO-1, and cytokeratin 18 in the MCF-7–derived cell lines undergoing EMT (Fig. 1A). These morphologic changes were also associated with a gain of mesenchymal markers. Indeed, SNAI1 transfection

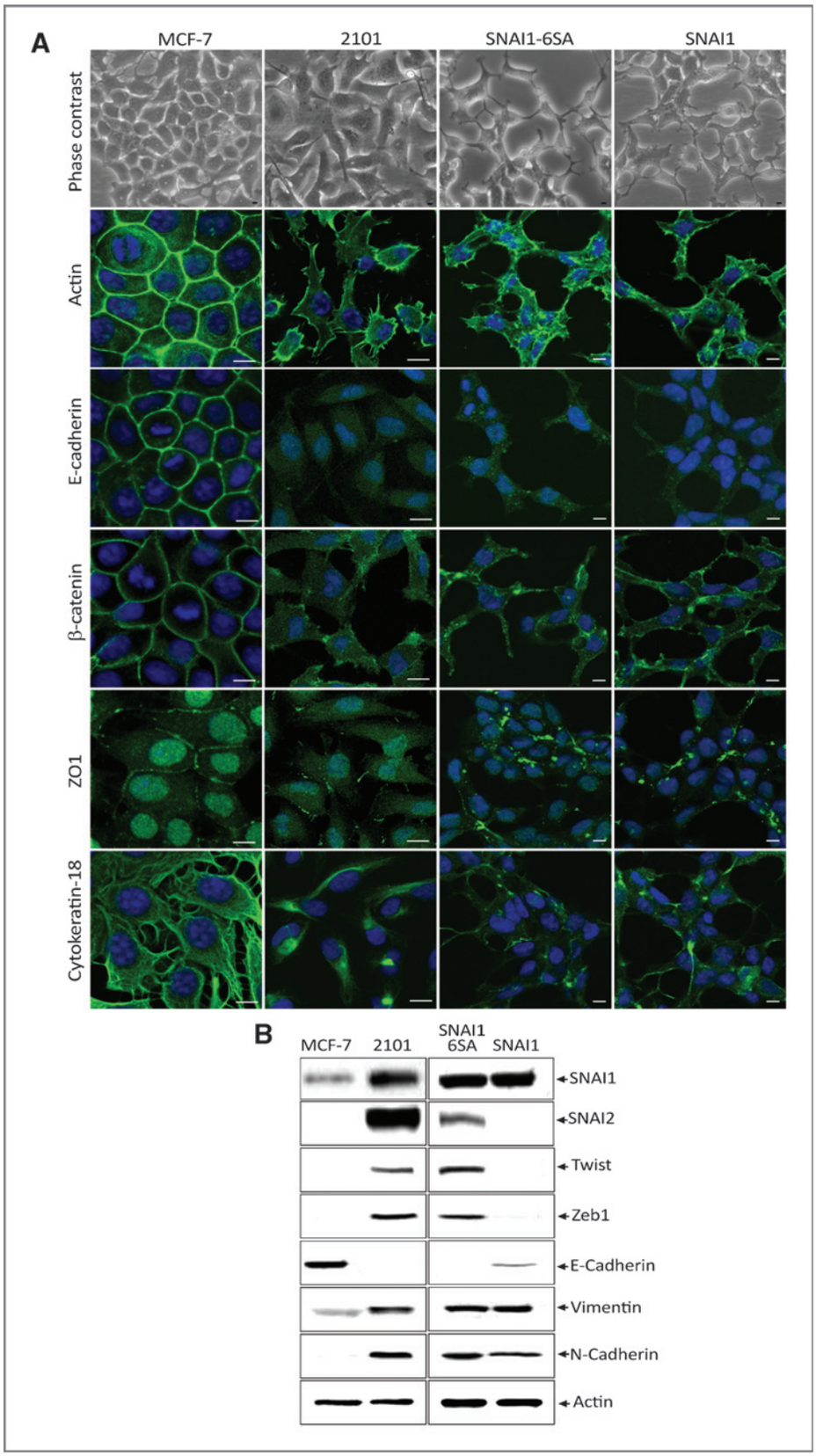

Figure 1. Differential expression of EMT markers in MCF-7 cell line and derived subclones. A, phase-contrast images showing the morphology of epithelial MCF-7 and mesenchymal derivative clones (2101, SNAI1-6SA, and SNAI1). Immunofluorescence staining of actin and epithelial markers (E-cadherin, β-catenin, ZO-1, and cytokeratin 18). Nuclei were stained with DAPI. B, Western blot analysis of the expression of EMT markers using the indicated antibodies.

induced the expression of N-cadherin and vimentin and decreased the expression of E-cadherin. SNAI1-6SA cells expressed SNAI2, ZEB1, but not E-cadherin (Fig. 1B). Thus, constitutively activated SNAI1-6SA cells are likely to exhibit a more pronounced mesenchymal-like phenotype than SNAI1 cells. Figure 1B also shows that 2101 cells exhibited a more complete EMT phenotype, with the expression of SNAI2, Twist, ZEB1, vimentin, and N-cadherin.

To provide further evidence for the EMT features of these cancer cell lines, we developed an EMT scoring method using gene expression profiling. As shown in Fig. 2A, an EMT score of -0.84 ± 0.008 was determined for the parental MCF-7 cells, indicating its well-known epithelial phenotype. As expected, SNAI1 cells acquired a mesenchymal-like phenotype; but the EMT score of -0.16 ± 0.007 instead indicated an intermediate phenotype. Similarly, the SNAI1-6SA cells were found to have an EMT score of -0.11 ± 0.01. In contrast, the 2101 cells scored a significantly higher 0.6 ± 0.02, which cannot be fully related to the Snail signature (60% concordance, data not shown) as other signatures, such as ZEB1, could contribute to this EMT score. This result suggests that 2101 cells acquire EMT by additional mechanisms that involve 2 or more transcriptional repressors of E-cadherin. It is worth noting that the acquisition of a resistance to TNF-α and the high EMT score in these 2101 cells suggest the existence of a level of complexity in the EMT process in which multiple molecules act together to mediate EMT, rather than the master regulators acting on their own. This indicates that EMT can be induced to varying degrees in epithelial cells to acquire intermediate mesenchymal-like states but also to display additional functional features. In this regard, Kim and colleagues have recently reported that p53 regulates EMT through miRNAs targeting ZEB1 and ZEB2 (21). It should be noted that 2101 cells display a mutated p53 and a loss of its transcriptional activity (13), which may, at least in part, account for the acquisition of EMT by these cells.

On the basis of the previously reported induction of stem cell markers following induction of EMT (22), we next determined the relationship between EMT score and stem cell characteristics such as $CD44^{high}/CD24^{low}$ profile and high ALDH activity. As shown in Fig. 2B, a, 2101 cells were equally partitioned into a $CD44^{high}$ and a $CD44^{-/low}$ populations as compared with MCF-7 cells, which displayed only a $CD44^{-}$ profile. Furthermore, measurements of ALDH activity showed a spectrum of high ALDH activity, with levels increasing in parallel to the estimated EMT score in MCF-7, SNAI1, SNAI1-6SA, and 2101 cells (Fig. 2B, b). Indeed, Fig. 2B(ii) shows that 2101 cells harbored the highest level of ALDH activity (92% $ALDH^{+}$) and MCF-7 cells the lowest (56% $ALDH^{+}$). Additional experiments showed an increased exclusion of the Hoechst dye, an increased expression of the stem cell markers SOX2, OCT4, NANOG, as well as spheroid formation and tumorigenicity in EMTed subclones (Supplementary Data S1). Consistent with these results, ZEB1 has been reported to link EMT activation and maintenance of stemness by suppressing stemness-inhibiting miRNAs (23). These results suggest that our EMTed clone exhibit stem cell–like properties.

Impairment of tumor cell susceptibility to CTL-mediated lysis upon EMT

To examine the functional consequences of target cell plasticity on specific T-cell–mediated lysis, we used the Heu33 CTL clone, which is able to lyse the parental MCF-7 cell line in an HLA-A2–restricted manner (11). As shown in Fig. 3A, a significant decrease in EMTed target cell susceptibility to CTL-mediated killing was observed. To determine whether impairment of T-cell–mediated lysis correlated with defects in recognition of Snail1-expressing cells, we examined conjugate formation between Heu33 CTL and MCF-7 cells or their derivative clones by confocal microscopy. The results shown in Fig. 3B, a indicate that MCF-7 parental cells were able to form stable conjugates with the Heu33 clone and could induce T-cell activation, as shown by an increase in tyrosine phosphorylation at the cell contact area. In contrast, a significant decrease of phosphotyrosine staining was detected when the CTL clone was cultured with mesenchymal cells (2101, SNAI1, and SNAI1-6SA), as confirmed by statistical analysis (Fig. 3B, b). The decrease in phosphotyrosine accumulation at the contact zone formed between mesenchymal and $CD8^{+}$ T cells reveals an alteration in the signaling events occurring at the immune synapse that may be potentially due to the expression of Snail. When reported as the percentage of active conjugates, a significant decrease in conjugates with phosphotyrosine accumulation was observed between the mesenchymal cells and $CD8^{+}$ T lymphocytes as compared with those observed between parental MCF-7 cell line and CTLs (Fig. 3B, c). As shown in Fig. 3C, mesenchymal tumor cells were less efficient in triggering cytokine production by CTL clone, indicating an influence of the EMT phenotype acquisition on T-cell reactivity.

Despite our increasing knowledge about tumor escape mechanisms, the involvement of EMT in tumor resistance to CTL-mediated killing and, in particular, how it counteracts effector T-cell responses has not been well documented. Here, we provide evidence that the acquisition of an EMTed phenotype results in the inhibition of target cell susceptibility to TCR-dependent lysis. In a previous study, we showed that resistance may be associated with morphologic changes (8). Our findings confirm that understanding the tumor behavior, especially in the context of tumor cell plasticity, and its interplay with effector cells will be key determinants in providing a rational approach to tumor immunotherapy. Accordingly, the various strategies aimed at the induction of antitumor cytotoxic responses should therefore consider the morphologic changes described in this report as an antitumor mechanism of tumor escape that is partly involved in resistance of cancer cells to CTL-mediated cytotoxicity.

EMT-induced tumor cell resistance to CTL-mediated lysis involves the induction of autophagy

We next asked whether EMT-dependent impairment of target cell susceptibility to CTL-mediated killing is associated with the activation of autophagy. Cells were transfected with GFP-LC3 to monitor the formation of autophagosomes. While no autophagosomes were detected in parental and control MCF-7 (MCF-7 and MCF-7 empty vector), the formation of autophagosomes (green dot–like structures) was observed in

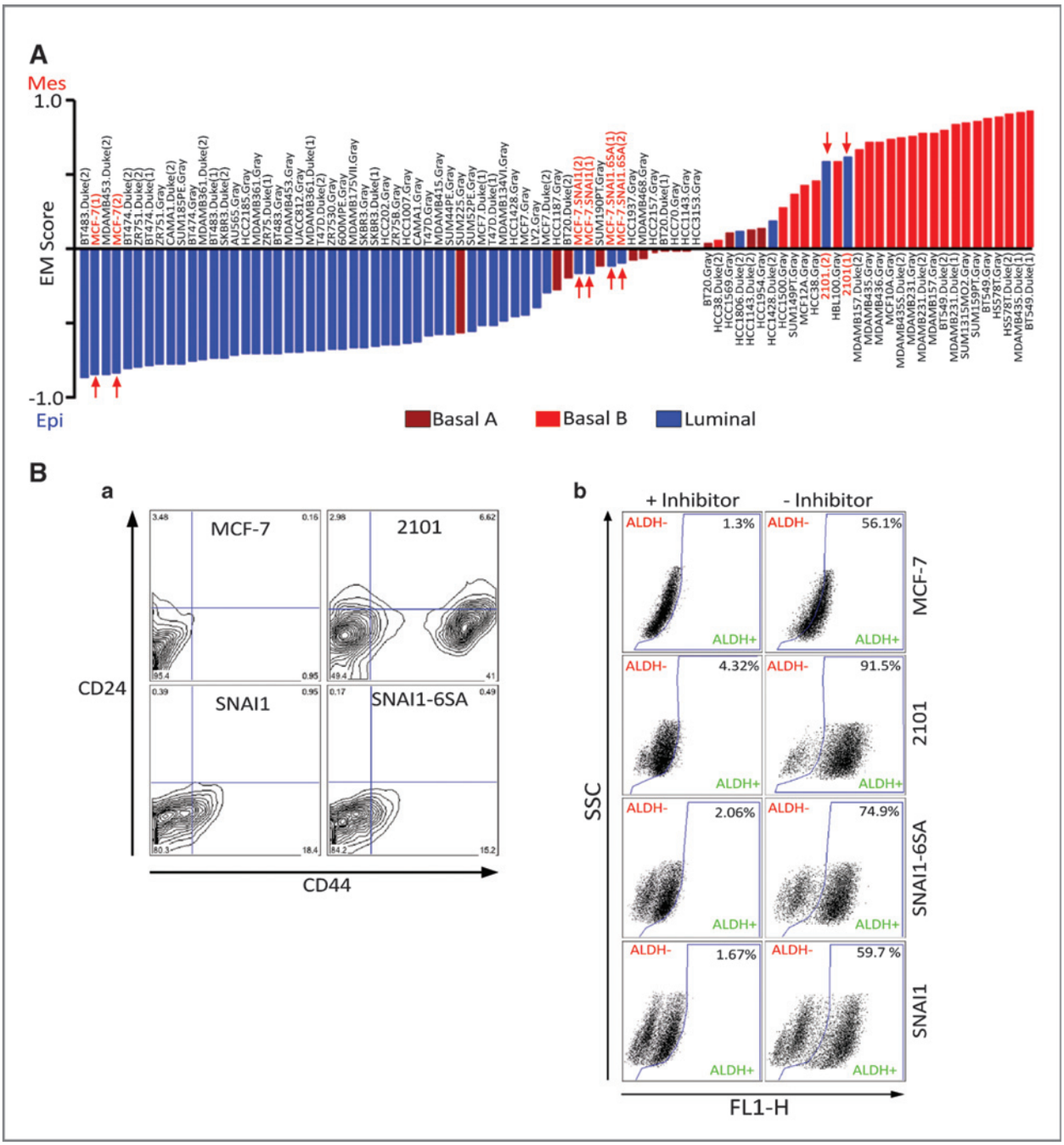

Figure 2. Differential EMT index is correlated with stem cell properties. A, EMT scores of cell lines. Underneath the bars is the corresponding breast cancer cell line name. B, impact of EMT-induced autophagy on cell surface markers of stemness and ALDH activity. a, contour plots are representative of CD44 and CD24 expression. b, identification of the $ALDH^{Low}$ and $ALDH^{High}$ populations. The +DEAB (inhibitor) control samples were used to set the gate where all cells were excluded. This gate was then applied to the −DEAB test sample, identifying the $ALDH^{High}$ population. The percentage of $ALDH^{High}$ cells is indicated at the top right corner. The Aldefluor assay was repeated at least 2 times for each cell line using a different passage at each time.

2101, SNAI1, and SNAI1-6SA cells (Fig. 4A). To analyze the autophagy flux, mesenchymal cells were treated with chloroquine, which induces the accumulation of autophagosomes and prevents their degradation by lysosomes. Figure 4B shows that, in the absence of chloroquine, there was an increase in both LC3-I and -II in the EMTed cells, suggesting autophagy induction in these cells. When mesenchymal cells were treated with chloroquine, there was an accumulation of LC3-II. Taken together, these data provide compelling evidence that autophagy flux is activated in cells undergoing EMT.

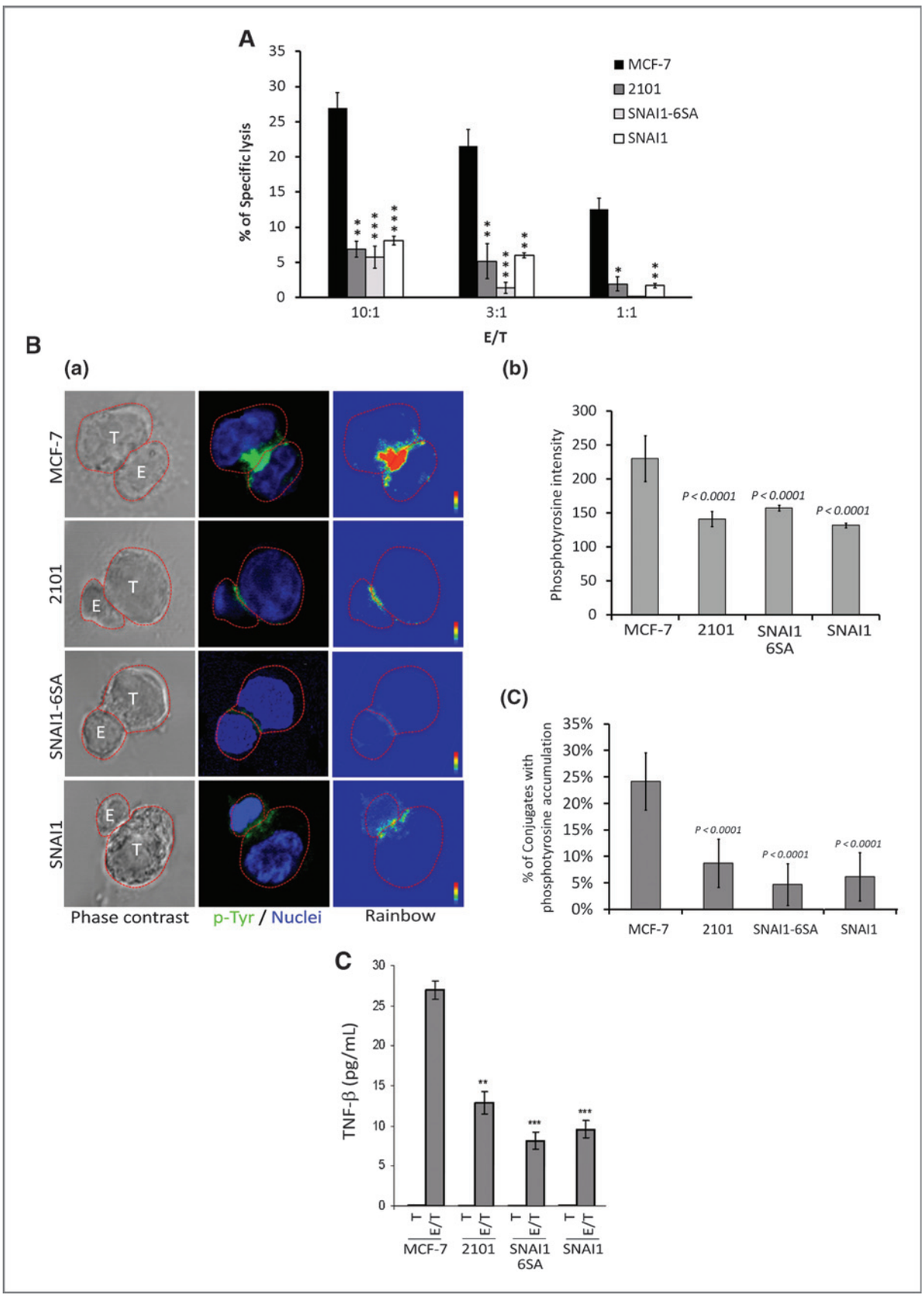

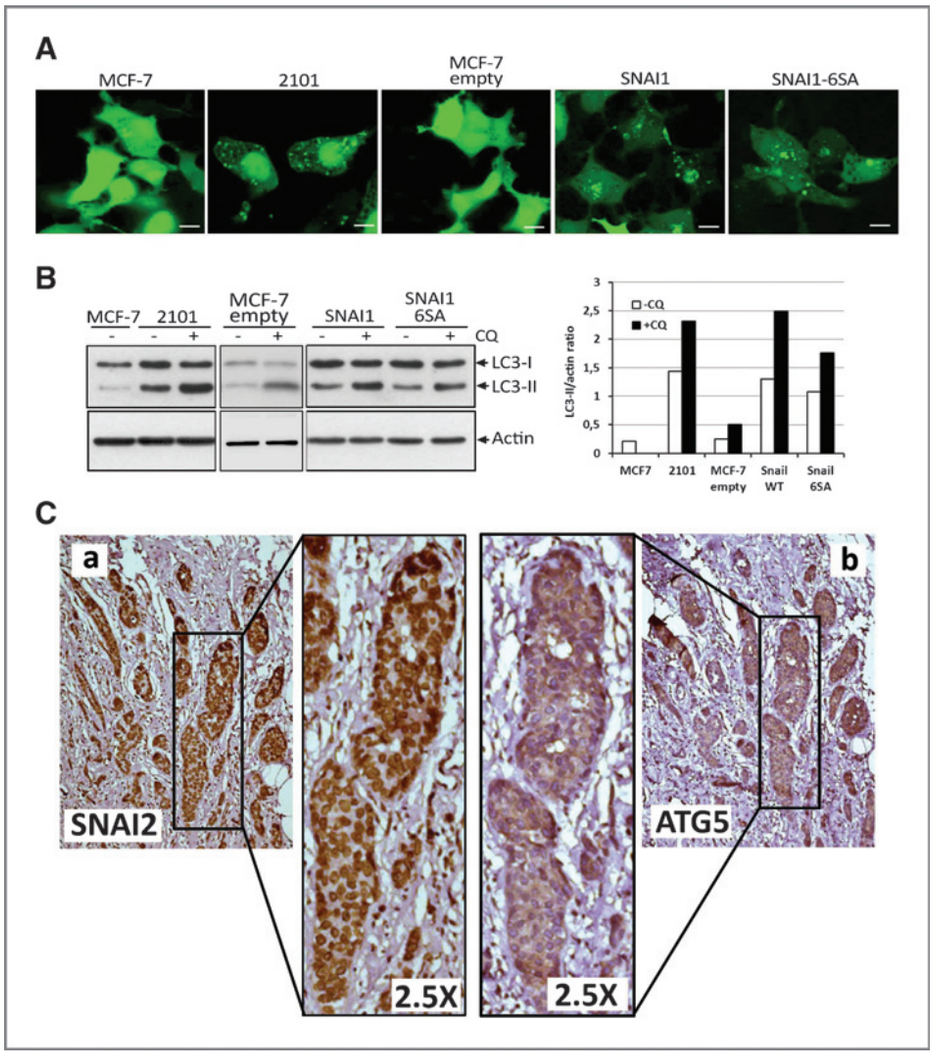

Figure 4. Autophagy flux in mesenchymal cell lines; coexpression of EMT and autophagy markers on human breast cancer serial tumor sections. A, formation of autophagosomes in GFP-LC3–expressing cells. Bar, 10 μm. B, left, Western blot analysis of the expression of autophagy markers LC3-I and -II in cells cultured in the absence (−) or presence (+) of chloroquine (CQ). Right, quantification of LC3-II/actin ratio of the Western blotting results. C, a and b, human breast cancer biopsies were stained for SNAI2 and ATG5 expression by immunohistochemistry on serial tumor sections.

Interestingly, the expression of the autophagy marker ATG5 was detected in human breast cancer tissues expressing the EMT marker SNAI2 (Fig. 4C, a and b). This figure shows clearly that ATG5 is localized in SNAI2-positive areas of tumors. As shown in Supplementary Data S5, the result of co-expression of EMT and autophagy markers in human breast cancer tissues was confirmed using another autophagy marker (LC3B). These findings suggest that EMT and autophagy markers co-express in human breast cancer tissues.

Inhibition of autophagy by targeting *beclin1* (Fig. 5A, a) sensitized mesenchymal tumor cells to CTL-mediated killing (Fig. 5A, b), which suggests that the process of EMT activates autophagy-dependent mechanisms to maintain tumor cell resistance to CTL. As EMTed ALDH$^+$-sorted cells were more resistant to the CTL-induced cell lysis (Supplementary Data S2), we suggest that the induction of autophagy and stem-like properties by the EMT program is critically important for the emergence of tumor cell resistant variants.

Data mining analysis was conducted to provide insight on how EMT regulates autophagy. Gene array results showed that the majority of autophagy core machinery genes (ATG) were not regulated at the transcriptomic level in Snail-expressing cells. BECN1 (ATG6) is the only ATG gene that was found to be significantly upregulated in 2101, SNAI1, and SNAI1-6SA, by approximately 2-fold. This supports the notion previously reported that autophagy machinery is not regulated at the

Figure 3. EMT decreases target cell susceptibility and reactivity to CTL clone. A, cytotoxicity was determined by a conventional 4-hour ^{51}Cr release assay at different ratios. Heu33 cells were used as effectors. Bars indicate SDs. B, (a), lack of phosphotyrosine accumulation at the immune synapse formed between T cells and mesenchymal cell lines (blue: nucleus; green: phosphotyrosine). quantification of phosphotyrosine intensity was conducted using the Region Measurements function of the ImageJ software (b). conjugates formed between T cells and tumor cells were scored by visual counting using a confocal microscope (c). Mean number of active synapses/field counted in 10 different fields/cell line were randomly selected. C, TNF-β production by the T-cell clone in response to tumor cell stimulation.

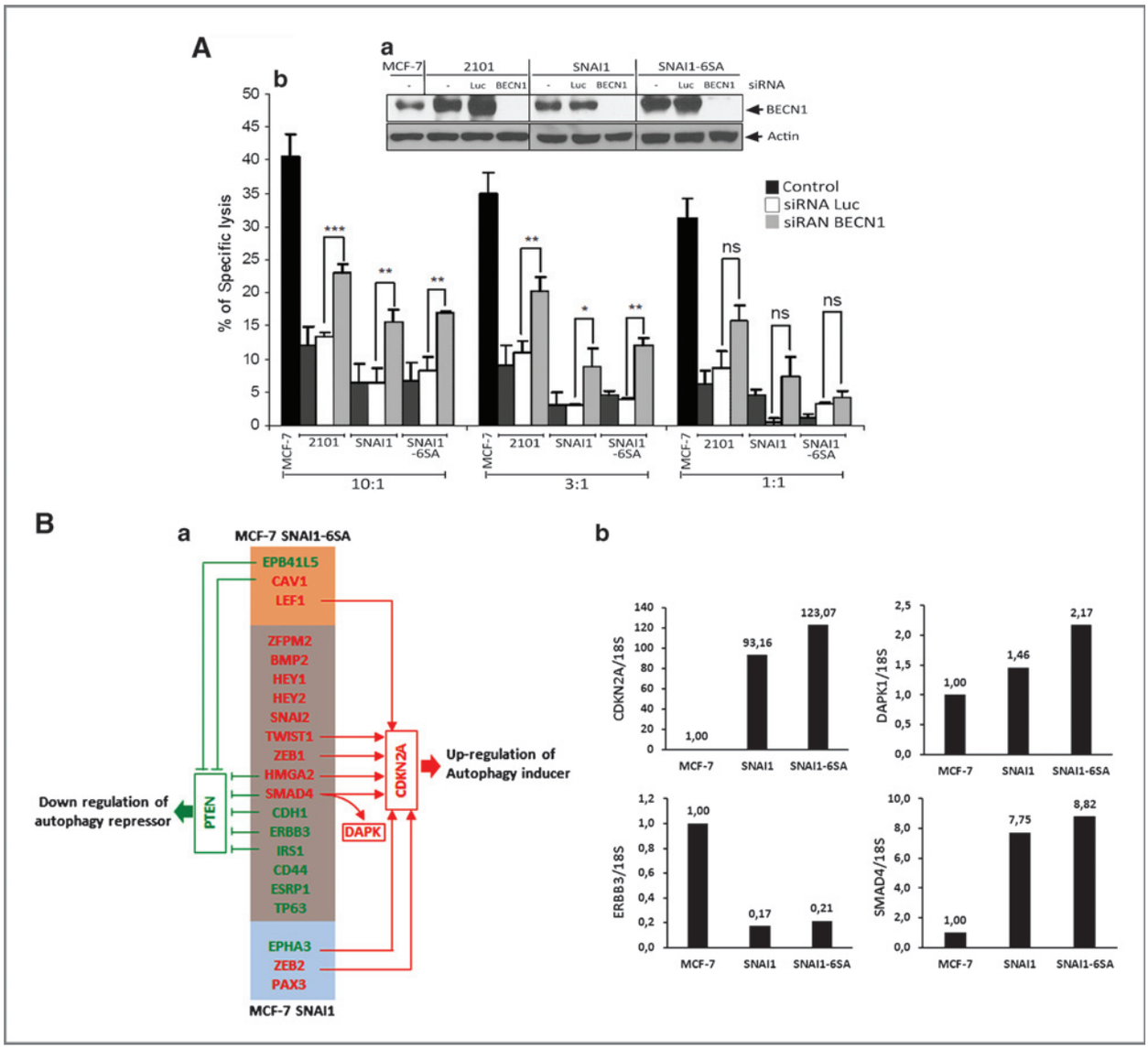

Figure 5. EMT-induced impairment of tumor cell susceptibility to CTL-mediated lysis is associated with the induction of autophagy. A, targeting EMT-induced autophagy restores mesenchymal tumor cells sensitivity to CTL-mediated lysis. Western blot analysis of the expression of beclin1 (BECN1) in untransfected cells and in cells transfected with either BECN1 or luciferase siRNAs (a). CTL-mediated cytotoxicity toward tumor cells at different E:T ratios (b). B, modulation of autophagy inducer and repressor genes in cells displaying an EMT phenotype. List of genes connecting EMT to autophagy (red, upregulated genes; green, downregulated genes; a). Real-time quantitative PCR (b) showing mRNA expression of selected genes involved in the induction/repression of autophagy. 18S was used as an endogenous control.

transcriptional level but mainly regulated by 3 types of post-translational modifications (phosphorylation, ubiquitylation, and acetylation; reviewed in ref. 24). As no transcriptional regulation of ATG genes involved in the core autophagy machinery was observed, we devoted more attention to the genes involved in the regulation of autophagy and thus identified DAPK1, PTEN, and CDKN2A. While the involvement of DAPK1 in the induction of autophagy is now well documented, PTEN and CDKN2A genes can regulate several cell functions, including cell cycle, apoptosis, and autophagy. Although much remains to be learned mechanistically, our result discloses for the first time a functional link between EMT and autophagy via PTEN and CDKN2A and thus paves the way for further investigations.

In conclusion, these data indicate that the acquisition of an EMT phenotype is an additional immune escape mechanism in tumor cells. Of interest, cells undergoing EMT acquired resistance to CTL-induced cell death, which reveals an insight into the significance of tumor cell plasticity and tumor resistance pathways. More importantly, the present work shows a relationship between EMT, autophagy, stem-like characteristics, and resistance of cancer cells to CTL-induced killing. This is the first report, using expression profiling, to show the molecular link between EMT and autophagy in cells displaying an EMT

phenotype. The in-depth analysis of the precise contribution of EMT transcription factors in autophagy regulation and how this homeostatic process is mechanistically linked to the maintenance of breast stem cell marker expression in tumor cells may improve our understanding of the relationship between EMT and tumor resistance to immune surveillance. These results indicate that reversing EMT to avoid immune resistance may represent a promising treatment strategy. Unraveling autophagy, a pharmacologically targeted mechanism, as an EMT-induced process could help to sensitize resistant EMTed cells to immunotherapy approaches.

Disclosure of Potential Conflicts of Interest

No potential conflicts of interest were disclosed.

Authors' Contributions

Conception and design: I. Akalay, B. Janji, M. Hasmim, M.Z. Noman, S. Chouaib
Development of methodology: I. Akalay, M. Hasmim, S. Chouaib
Acquisition of data (provided animals, acquired and managed patients, provided facilities, etc.): M. Hasmim, M.Z. Noman, F. Andre, P. Bertheau, C. Badoual, A.K. Larsen, N.T.Y. Hung, J.P. Thiery, S. Chouaib
Analysis and interpretation of data (e.g., statistical analysis, biostatistics, computational analysis): I. Akalay, B. Janji, M. Hasmim, F. Andre, P. De Cremoux, T.Z. Tan, J.H. Keira, S. Chouaib
Writing, review, and/or revision of the manuscript: I. Akalay, B. Janji, M. Hasmim, M.Z. Noman, F. Andre, C. Badoual, P. Vielh, A.K. Larsen, M. Sabbah, J.P. Thiery, M. Mami-Chouaib, S. Chouaib
Administrative, technical, or material support (i.e., reporting or organizing data, constructing databases): M. Mami-Chouaib, S. Chouaib
Study supervision: S. Chouaib

Acknowledgments

The authors thank Prof. Mien-Chie Hung at the MD Anderson Cancer Center for providing the MCF-7 (WT and SNAI1-6SA) cell lines.

Grant Support

This work was supported by grants from INSERM, la Ligue Nationale Contre le Cancer, Luxembourg Ministry of Culture, Higher Education and Research (Grant 2009 0201), A*STAR Institute of Molecular Cell Biology and Cancer Science Institute National University of Singapore core grants.

Received June 26, 2012; revised January 24, 2013; accepted January 25, 2013; published OnlineFirst February 22, 2013.

References

1. Rosenberg SA. Progress in the development of immunotherapy for the treatment of patients with cancer. J Intern Med 2001;250:462–75.
2. Chouaib S, Asselin-Paturel C, Mami-Chouaib F, Caignard A, Blay JY. The host-tumor immune conflict: from immunosuppression to resistance and destruction. Immunol Today 1997;18:493–7.
3. Kiessling R, Wasserman K, Horiguchi S, Kono K, Sjoberg J, Pisa P, et al. Tumor-induced immune dysfunction. Cancer Immunol Immunother 1999;48:353–62.
4. Anichini A, Molla A, Mortarini R, Tragni G, Bersani I, Di Nicola M, et al. An expanded peripheral T cell population to a cytotoxic T lymphocyte (CTL)-defined, melanocyte-specific antigen in metastatic melanoma patients impacts on generation of peptide-specific CTLs but does not overcome tumor escape from immune surveillance in metastatic lesions. J Exp Med 1999;190:651–67.
5. Chouaib S. Integrating the quality of the cytotoxic response and tumor susceptibility into the design of protective vaccines in tumor immunotherapy. J Clin Invest 2003;111:595–7.
6. Kudo-Saito C, Shirako H, Takeuchi T, Kawakami Y. Cancer metastasis is accelerated through immunosuppression during Snail-induced EMT of cancer cells. Cancer Cell 2009;15:195–206.
7. Onder TT, Gupta PB, Mani SA, Yang J, Lander ES, Weinberg RA. Loss of E-cadherin promotes metastasis via multiple downstream transcriptional pathways. Cancer Res 2008;68:3645–54.
8. Abouzahr S, Bismuth G, Gaudin C, Caroll O, Van Endert P, Jalil A, et al. Identification of target actin content and polymerization status as a mechanism of tumor resistance after cytolytic T lymphocyte pressure. Proc Natl Acad Sci U S A 2006;103:1428–33.
9. Lavieu G, Scarlatti F, Sala G, Levade T, Ghidoni R, Botti J, et al. Is autophagy the key mechanism by which the sphingolipid rheostat controls the cell fate decision? Autophagy 2007;3:45–7.
10. Yang J, Weinberg RA. Epithelial-mesenchymal transition: at the crossroads of development and tumor metastasis. Dev Cell 2008;14:818–29.
11. Dorothee G, Echchakir H, Le Maux Chansac B, Vergnon I, El Hage F, Moretta A, et al. Functional and molecular characterization of a KIR3DL2/p140 expressing tumor-specific cytotoxic T lymphocyte clone infiltrating a human lung carcinoma. Oncogene 2003;22:7192–8.
12. Zhou BP, Hu MC, Miller SA, Yu Z, Xia W, Lin SY, et al. HER-2/neu blocks tumor necrosis factor-induced apoptosis via the Akt/NF-kappaB pathway. J Biol Chem 2000;275:8027–31.
13. Cai Z, Capoulade C, Moyret-Lalle C, Amor-Gueret M, Feunteun J, Larsen AK, et al. Resistance of MCF7 human breast carcinoma cells to TNF-induced cell death is associated with loss of p53 function. Oncogene 1997;15:2817–26.
14. Johnson WE, Li C, Rabinovic A. Adjusting batch effects in microarray expression data using empirical Bayes methods. Biostatistics 2007;8:118–27.
15. Gatza ML, Lucas JE, Barry WT, Kim JW, Wang Q, Crawford MD, et al. A pathway-based classification of human breast cancer. Proc Natl Acad Sci U S A 2010;107:6994–9.
16. Verhaak RG, Hoadley KA, Purdom E, Wang V, Qi Y, Wilkerson MD, et al. Integrated genomic analysis identifies clinically relevant subtypes of glioblastoma characterized by abnormalities in PDGFRA, IDH1, EGFR, and NF1. Cancer Cell 2010;17:98–110.
17. El Hage F, Stroobant V, Vergnon I, Baurain JF, Echchakir H, Lazar V, et al. Preprocalcitonin signal peptide generates a cytotoxic T lymphocyte-defined tumor epitope processed by a proteasome-independent pathway. Proc Natl Acad Sci U S A 2008;105:10119–24.
18. Magnon C, Opolon P, Ricard M, Connault E, Ardouin P, Galaup A, et al. Radiation and inhibition of angiogenesis by canstatin synergize to induce HIF-1alpha-mediated tumor apoptotic switch. J Clin Invest 2007;117:1844–55.
19. HADb. Human Autophagy Database. www.autophagy.lu.
20. Moussay E, Kaoma T, Baginska J, Muller A, Van Moer K, Nicot N, et al. The acquisition of resistance to TNFalpha in breast cancer cells is associated with constitutive activation of autophagy as revealed by a transcriptome analysis using a custom microarray. Autophagy 2010;7:760–70.
21. Kim T, Veronese A, Pichiorri F, Lee TJ, Jeon YJ, Volinia S, et al. p53 regulates epithelial-mesenchymal transition through microRNAs targeting ZEB1 and ZEB2. J Exp Med 2011;208:875–83.
22. Mani SA, Guo W, Liao MJ, Eaton EN, Ayyanan A, Zhou AY, et al. The epithelial-mesenchymal transition generates cells with properties of stem cells. Cell 2008;133:704–15.
23. Wellner U, Schubert J, Burk UC, Schmalhofer O, Zhu F, Sonntag A, et al. The EMT-activator ZEB1 promotes tumorigenicity by repressing stemness-inhibiting microRNAs. Nat Cell Biol 2009;11:1487–95.
24. McEwan DG, Dikic I. The Three Musketeers of autophagy: phosphorylation, ubiquitylation and acetylation. Trends Cell Biol 2011;21:195–201.